J Nanostruct 13(3): 783-795, Summer 2023

RESEARCH PAPER

Enhanced Adsorption of Malachite Green Using Carboxymethyl Cellulose/Carboxylic-Multiwall Carbon Nanotube Hybrid Hydrogel Nanocomposite

Zainab R. Maktof [1], *and Nadher D. Radia* [2] *

[1] *Thi-Qar General Directorate of Education, Ministry of Education, Thi-Qar, Iraq*

[2] *Department of Chemistry, College of Education, University of Al-Qadisiyah, Al-Qadisiyah, Iraq*

ARTICLE INFO

Article History:
Received 09 April 2023
Accepted 17 June 2023
Published 01 July 2023

Keywords:
Carboxylic-Multiwall Carbon Nanotube
Enhanced Adsorption
Malachite Green
Nanocomposite

ABSTRACT

Synthesis and investigation of a sodium carboxymethyl cellulose grafting poly (acrylic acid) hydrogel (NaCMC-g-pAAc) and a sodium carboxymethyl cellulose grafting poly (acrylic acid)/carboxylic multiwalled carbon nanotubes hydrogel nanocomposite (NaCMC-g-pAAc\COOH-MWCNTs nanocomposite hydrogel) as malachite green (MG) dye adsorbents was undertaken in this study. The grafting reaction integrated a certain weight of oxidized COOH-MWCNTs into the hydrogel matrix through the copolymerization of acrylic acid AAC onto sodium carboxymethyl cellulose (NaCMC). The resulting optimal hydrogel, with its maximum swelling capacity, was further combined with oxidized MWCNTs to form NaCMC-g-pAAc\COOH-MWCNTs, displaying a swelling capacity peak of 1800% at pH 7.0. The NaCMC-g-pAAc and NaCMC-g-pAAc\COOH-MWCNTs' structure, thermal stability, and morphology were characterized utilizing techniques such as fourier transform infrared (FTIR), x-ray diffraction (XRD), TGA, and scanning electron microscopy (FE-SEM). Batch-wise investigations of the effects of pH, equilibrium time, weight, and salt on MG dye adsorption were conducted. Adsorbent's negatively charged groups (COOH) were generated at an optimal pH 7, which established a strong interaction with MG's positive charges, reaching adsorption equilibrium in 120 min. The adsorption potential of the NaCMC-g-PAA/COOH-MWCNTs hydrogel nanocomposite for MG was remarkably high, recorded at 198.8173 mg/g at 25°C. A suitable match for the dye adsorption data was found to be provided by both the pseudo-second-order model and the Freundlich model.

How to cite this article
Maktof. R., Radia N. D. Enhanced Adsorption of Malachite Green Using Carboxymethyl Cellulose/Carboxylic-Multiwall Carbon Nanotube Hybrid Hydrogel Nanocomposite. J Nanostruct, 2023; 13(3):783-795. DOI: 10.22052/JNS.2023.03.019

INTRODUCTION

The recent surge in industries such as textiles and printing has caused a substantial increase in organic dye wastewater production. The environmental issues posed by these organic dyes are due to their high solubility, non-biodegradability, and carcinogenic properties [1-4]. Accordingly, research into efficient dye removal from wastewater has gained significant attention. The most favored method is adsorption, thanks to its simple, cost-effective, efficient, and reusable nature [5,11]. Carbon nanotubes (CNTs),

* *Corresponding Author Email: nadhir.dhaman@qu.edu.iq*

because of their excellent properties and potential for functionalization, are considered optimal adsorbents [12-16]. In literature, successful adsorption of dyes such as methyl orange (MO) and methylene blue (MB) has been documented, employing pristine multi-walled carbon nanotubes (MWCNTs) as the adsorptive medium [3,11]. Despite this, the hydrophobic nature of CNTs and the strong forces between them cause entanglement and clumping in aqueous solutions, thereby limiting their adsorption efficiency. To overcome this, CNTs have been modified using physical or chemical methods Physical methods can improve dispersion but often cause significant structural damage. Thus, chemical modifications, which enhance CNT hydrophilicity without damaging their structure, are typically favored [Such modifications not only improve hydrophilicity but also create more adsorption sites for dye molecules. The effectiveness of dye adsorption is usually determined by various interaction forces. Despite existing research on the adsorption kinetics and isotherms for dyes on modified MWCNTs, a comprehensive understanding of interaction forces and adsorption mechanisms remains limited [17-20]. Therefore, this paper aims to detail the adsorption properties and mechanisms of dye removal on adsorbents. Hydrogels, based on biopolymers, have garnered distinct attention as optimal adsorbents, given their application across various domains, such as healthcare, drug delivery, cosmetics, agriculture, and wastewater treatment. Their appeal for the absorption of synthetic dyes from polluted water is underlined by their considerable adsorption capacities, recoverability, and repeatably regenerative capabilities. Recent times have witnessed a heightened focus on hydrogel development, particularly hydrogel-nanoparticle composites, due to their enhanced mechanical/thermal resilience and swelling properties compared to non-additive hydrogels. This has established the field of nanoscale hydrogel composite engineering as an attractive global research area. Various strategies have been explored to develop nanoscale hydrogel composites, involving a range of nanoparticles like carbon-based, montmorillonite, polymeric, ceramic, and metallic nanomaterials [21].

In this study, MWCNTs were modified with an acrylic acid (AAc) monomer onto sodium carboxymethyl cellulose (NaCMC) to create nanocomposite hydrogels. AAc grafting on COOH-MWCNTS is increased by minimizing the polymer chain's steric hindrance impact. FTIR, XRD, and TGA were used to characterize the nanocomposite hydrogels' surface morphology, chemical composition, elemental content, structural defects, component content, and hydrophilicity. Malachite Green (MG) dye was removed from aqueous solutions using the NaCMC-g-pAAc\ COOH-MWCNTs nanocomposite hydrogel as an adsorbent. pH, adsorption period, solution concentration, and temperature were examined to determine how this affected adsorbent performance.

MATERIALS AND METHODS

Materials

This study included sodium carboxymethyl cellulose (NaCMC) 99%, acrylic acid (AAc) 99%, oxidized Multi-Walled Carbon (COOH-MWCNTs), N,N-methylenebisacrylamide (MBA) 98%, potassium persulfate (KPS) (98%), Malachite Green (MG), hydrochloric acid (HCl) 97%, and sodium hydroxide (NaOH). All were from Merck. Analytical-grade reagents didn't need purification. Analytical purity was achieved by utilizing deionized water to produce solutions.

Synthesis (NaCMC-g-pAAc) hydrogel (NaCMC-g-pAAc/COOH-MWCNTs nanocomposite hydrogel)

In this procedure, 1g of sodium Carboxymethyl Cellulose (NaCMC) was dissolved in 25 mL of deionized (DI) water. Subsequently, 1.5g of Acrylic Acid (AAc) was added to the solution in a periodic manner. A solution containing N,N-methylenebisacrylamide (MBA) and potassium persulfate (KPS) was prepared by dissolving 0.075g of MBA and 0.05g of KPS in 2 mL of distilled water each. This solution was added to the initial mixture under vigorous stirring, keeping the total volume at 31 mL. Meanwhile, 0.004g of oxidized Multi-Walled Carbon Nanotubes (COOH-MWCNTs) were sonicated in 2 mL of DI water for about 60 minutes. This solution was then introduced into the reaction mixture containing CMC, AAc, MBA, and KPS, still under continuous stirring, with a final reaction volume kept at 30 mL. The reaction was conducted at 70°C for 3 hours in a water bath. The resultant product was cut into small pieces, washed with DI water to remove any unreacted substances, and then dried in an oven at 70°C for about 24 hours. The dried product (NaCMC-g-pAAc/COOH-MWCNTs nanocomposite hydrogel)

was subsequently ground into a fine powder, as depicted in Fig. 1.

Characterizations (NaCMC-g-pAAc and (NaCMC-g-pAAc)/COOH-MWCNTs Composite

The functional group classifications of sodium carboxymethyl cellulose grafted poly (acrylic acid) (NaCMC-g-pAAc) hydrogel and NaCMC-g-pAAc COOH-MWCNTs nanocomposite hydrogel were assessed by Fourier Transform Infrared Spectroscopy (FTIR) (Shimadzu8400S, Japan). Surface data were captured in a wavelength range of 4000-400 cm^{-1} using potassium bromide (KBr) [25]. The morphological features of the nanocomposite hydrogel, inclusive of size and shape, were examined before and after the loading of malachite green (MG) dye using Field Emission Scanning Electron Microscopy (FE-SEM) with varied magnification powers [26]. The crystalline characteristics of the hydrogel and nanocomposite were analyzed through the XRD (Shimadzu XRD-6000, Japan) method using CuK light of a single wavelength (1.5104 A). The Thermogravimetric Analysis (TGA) technique was employed to inspect the physical and chemical properties of NaCMC-g-pAAc hydrogel and NaCMC-g-pAAc/COOH-MWCNTs nanocomposite hydrogel by tracking mass alterations during slow, steady heating from 50 to 800°C under nitrogen gas conditions. Lastly, the Ultraviolet-visible spectrophotometer (UV-vis) was used to evaluate the MG dye concentration post-adsorption at a wavelength of 625.5 nm.

Kinetic Studies

The influence of interaction duration was examined by introducing 0.05 g of the adsorbent into a 10 mL dye solution, featuring an initial concentration of 1000 $mg.L^{-1}$, under agitated conditions. The solution's temperature was consistently maintained at 25 ºC using a thermostatic shaker. Post specified time intervals, the solutions underwent centrifugation, with 3 mL aliquots of the supernatant being subsequently extracted for spectrophotometric evaluations of dye content.

Swelling Studies

In order to delve into the nature of hydrogel swelling properties, a comprehensive study was undertaken, wherein 100 mg of the samples were meticulously submerged in approximately 80 mL of different pH, all the while maintaining a temperature of 25°C, for a duration of 48 h. Upon completion of the immersion period, the swollen samples were delicately extracted from the aqueous solution and any superfluous water residing on the surface was cautiously eradicated, followed by a re-weighing of the samples so as to determine the extent of their swelling percentage. The swelling percentage (S%) of the samples was then diligently calculated using aq (1).

$$S\% = \frac{W_s - W_d}{W_d} * 100 \quad (1)$$

the weight of the initial dry sample, represented by W_d, and the weight of the swollen hydrogel sample, represented by W_s.

Adsorption Studies

The absorption tendencies of MG dye onto CMC-g-pAAc/COOH-MWCNTs nanocomposite hydrogel were examined in a batch configuration. Adsorption experiments were conducted with 10 ml of MG dye solution utilizing 0.05g of adsorbents, undergoing agitation in a thermoregulated shaker set to 120 rpm over a defined duration. Subsequently, dye-laden solutions were isolated,

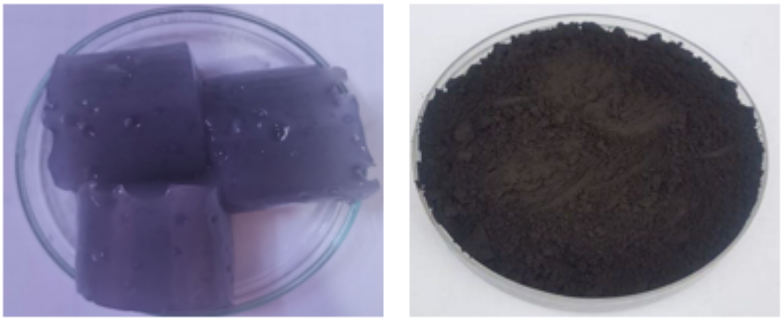

Fig. 1. (NaCMC-g-pAAc/COOH-MWCNTs nanocomposite hydrogel

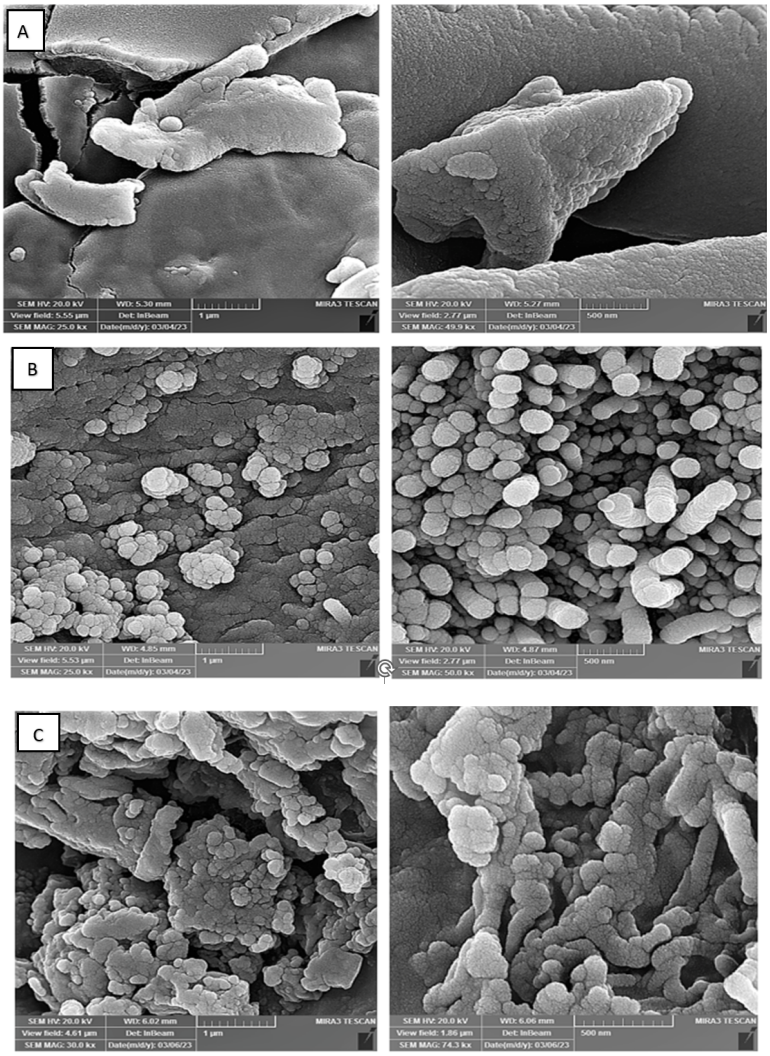

Fig. 2. SEM images of (A)(NaCMC-pAAc) hydrogel (B) (NaCMC-g-pAAc)/COOH-MWCNTs nanocomposite hydrogel (C) (NaCMC-g-pAAc)/COOH-MWCNTs nanocomposite hydrogel after Adsorption of MG dye

and a centrifuge mechanism was employed for fluid separation. The impact of initial pH on MG adsorption was evaluated, with the effect of pH on adsorption capacity spanning from 3.0 to 10.0. The dose-dependent effect of the adsorbent on the adsorption capacity was assessed using 0.05g. For kinetic studies of adsorption, the contact time was adjusted to 120 minutes. Adsorption isotherm trials saw MG dye concentrations ranged from 100 to 1000 mg/l. The effects of interaction time and equilibrium concentration were assessed at 25°C. Upon completion of the adsorption process, the aliquots were centrifuged, and the concentration determined using the UV-vis spectrophotometer (Shimadzu8400S, Japan) at a λmax of 625.5 nm for the MG dye. Adsorption percentages and adsorption capacity (qe) were calculated via Eqs(2,3) respectively.

$$Adsorption\% = \left(\frac{C\,0\ * Ce}{C0}\right) * 100 \tag{2}$$

$$qe\left(\frac{mg}{g}\right) = qt = \left(\frac{C0 - Ce}{m}\right) v \tag{3}$$

where q_t (mg/g) represents the amount of MG adsorbed per unit mass of the adsorbent at a certain time (t). C_e (mg/L) is the equilibrium concentration of MG, m (g) is the mass of the

adsorbent, and $V_{(L)}$ is the volume of the MG dye solution.

RESULTS AND DISCUSSION

The scanning electron microscopy technique (FESEM) was used to study the surface properties of the prepared materials, through which the shape of the particles, their size, and the nature of their aggregations among themselves, in addition to the nature of the surfaces, are identified. In terms of whether it is porous or soft, as well as knowing the amount of homogeneity between the components and their distribution on the surface. Regarding the Field Emission Scanning Electron Microscope (SEM-FE) images of the hydrogel (CMC-g-pAAc) and its composite (CMC-g-pAAc/COOH-MWCNTs), they reveal a smooth, clear, and porous surface of the hydrogel. This is characterized by a sponge-like structure and a compact network, credited to the strong binding of the crosslinking agent with polymer chains. However, upon addition of COOH-MWCNTs to the gel, leading to superposition, the surface exhibits increased roughness and porosity along with an irregular structure. A homogeneous dispersion of COOH-MWCNTs is observed throughout the hydrogel matrix, with no visible aggregations, attributable to the aggregates' functionalization on both COOH-MWCNTs and hydrogel surfaces [22]. Considering the MG dye adsorption on the composite surface, the SEM-FE images display enhanced surface smoothness resulting from the dye particles completely filling the pores and forming a layer. This implies a surface fully coated with dye particles, affirming the adsorption process (Fig. 2) [23].

Presented in Fig. 3a (i) is the Fourier Transform Infrared Spectroscopy (FTIR) data for NaCMC,

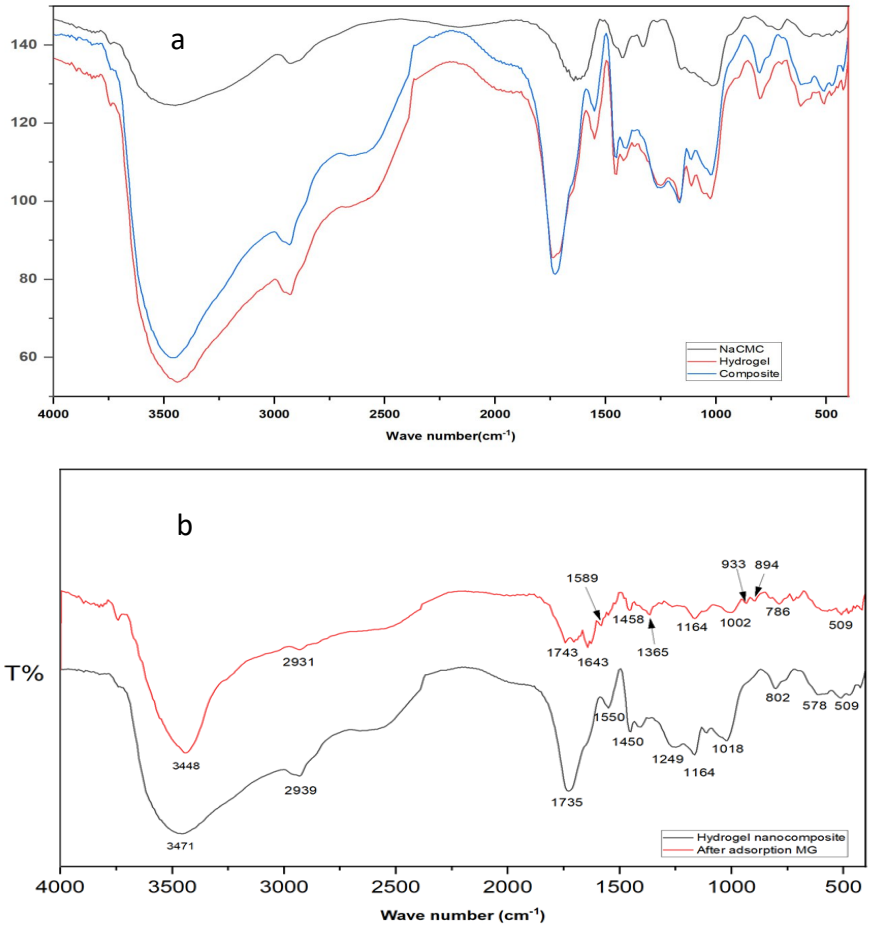

Fig. 3. a) FT-IR of (i) NaCMC (ii) hydrogel (iii) hydrogel nanocomposite, b) FT-IR of hydrogel nanocomposite and after adsorption MG

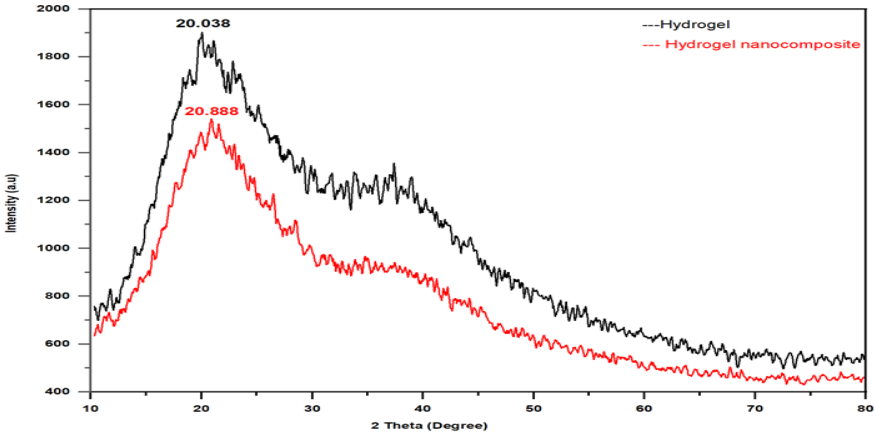

Fig. 4. XRD pattern Hydrogel and nanocomposite hydrogel

which reveals a broad absorption peak at 3319 cm^{-1}, signaling the presence of hydrogen-bonded O-groups. Absorption bands witnessed at 1718, 1460, and 1402 cm^{-1} are attributable to the stretching vibration of the C=O from the carboxylate group. Polysaccharide-associated absorption bands also emerge at 1410 cm^{-1} and 1023 cm^{-1}, linked to C–H bending and CO bond stretching, respectively [29]. With respect to NaCMC-pAAc hydrogel and NaCMC-pAAc/COOH-MWCNTs, an amplification of the characteristic band's intensity at 1402 cm^{-1} is noticed, hinting at the symmetric stretching mode of the carboxylate group and corroborating the formation of the hydrogel. Additional peaks at 1537 cm^{-1} were related to the C=O asymmetric stretching of carboxylate anions in AA units. Additionally, a broad absorption peak at 3319 cm^{-1} for NaCMC evolved into a hump at 3142 cm^{-1} in the broad absorption peak after AA surface modification [24]. These findings suggest successful AA copolymer grafting onto the CMC [Fig. 3a (ii) and (iii)].

For NaCMC-pAAc hydrogel and NaCMC-pAAc/COOH-MWCNTs hydrogel nanocomposite, similar characteristic peaks were noted. The actual peaks for COOH-MWCNTs were not visible in the NaCMC-pAA/COOH-MWCNTs hydrogel nanocomposite case, indicating possible signal overlay by NaCMC-pAAc signals due to interactions between COOH-MWCNTs chains and CMC-pAAc chains. The FTIR spectrum of NaCMC-pAAc hydrogel and NaCMC-pAAc/COOH-MWCNTs post-MG dye adsorption reveals a peak at 3471 cm^{-1}, corresponding to the $-NH_2$ group of aliphatic and aromatic groups in MG. The characteristic bands' intensities at 2858 and 2927 cm^{-1} were attributed to the stretching vibration of −CH aromatic and $-CH_3$ methyl groups of MG [31] [Fig. 3b]. This confirms MG interaction with NaCMC-pAAc and NaCMC-pAAc/COOH-MWCNTs.

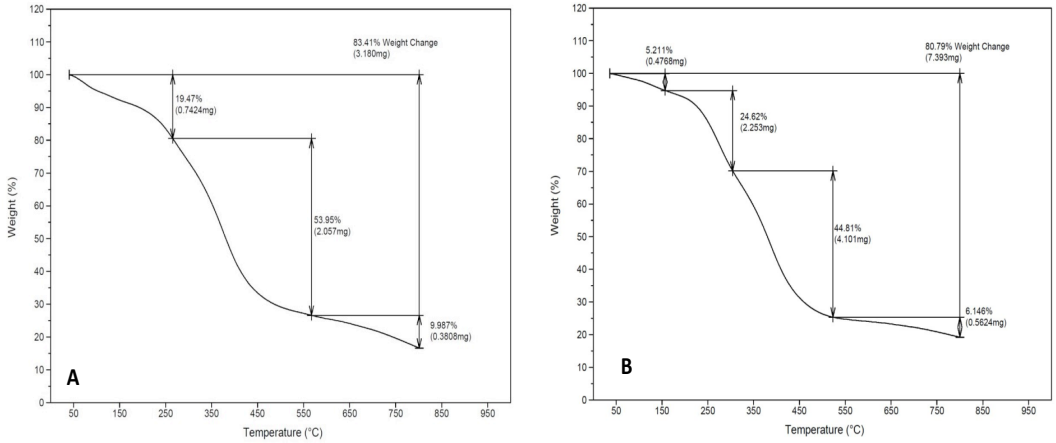

Fig. 5. TGA of Hydrogel and nanocomposite hydrogel

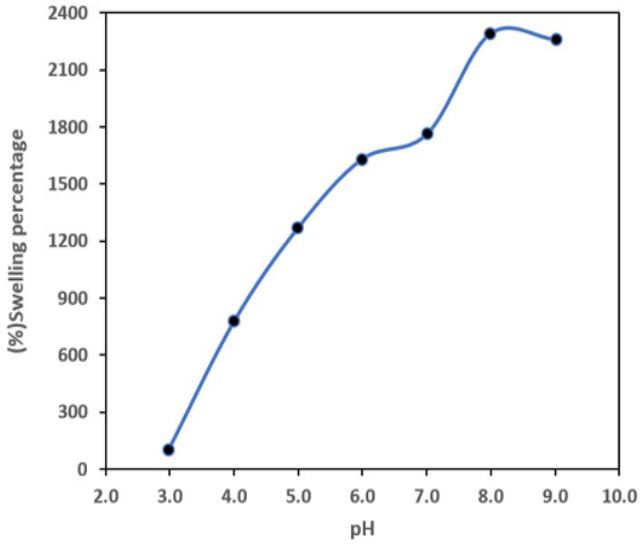

Fig. 6. Swelling of the hydrogels at various pHs at 25°C

Further, the X-ray diffraction (XRD) spectra for the NaCMC-g-pAAc hydrogel and its composite with NaCMC-pAAc/COOH-MWCNTs (Fig. 4) display a broad band in the 2θ (15-30) angular range. This hints at the amorphous character of the crosslinked chemical structure found in both the hydrogel and its nanocomposite. Specifically, the XRD spectrum of the aqueous gel presents a broad band at (2θ = 20.038), while the corresponding band for the nanocomposite appears at (2θ = 20.888) [25].

The Thermogravimetric Analysis (TGA) curve for the hydrogel [Fig. 5(a-b)] uncovered three stages of incremental weight loss as the temperature rose. The initial stage involves a weight loss of (19.47%) between (50-250C) due to water residual loss. The second stage with a loss of (53.95%) between (250-550C), resulted from CMC degradation and residue carbide form. The final stage with a loss of (9.987%) between (550-800C), could be due to the breaking of carboxyl groups from acrylic acid. The TGA curve for the (CMC-g-pAAc)/COOH-MWCNTs.

The water absorption of NaCMC-g-pAAc/COOH-MWCNTs hydrogels was investigated in the pH range 3.0–9.0 (Fig. 6). The results of the swelling studies showed that it has a pH-dependent behavior. Moreover, the absorbent showed similar water absorption trends throughout the studied pH range. In acidic conditions, the pipette showed little swelling. It was observed that an increase in solution pH increased the swelling ability of NaCMC-g-pAAc/COOH-MWCNTs. The maximum swelling ratio observed is 2,268.4% at pH 8.0 for NaCMC-g-pAAc/COOH-MWCNTs. At alkaline pH, the lattice structure showed extensive swelling in the aqueous medium due to the presence of hydrophilic groups, i.e., -COOH, which renders the negative charge density involved in electrostatic interactions with water molecules. Hydrophilic nanocomposites embedded in COOH-MWCNTs showed greater swelling capabilities than hydrophilic polymeric matrices. The swelling degree of NaCMC-g-pAAc/COOH-MWCNTs was relatively high, which was due to the low conformational strength. It is well established that the improvement in gel strength is inversely proportional to the degree of swelling. Therefore, the results of the swelling studies support the results of the mechanistic studies [26]

With a fixed concentration of 1000 ppm MG dye, several weights of the prepared hydrogel complex, ranging from g (0.01-0.15), were obtained, and 10 ml of the dye solution was added to the weights prepared at 25°C. The weight of the adsorbent increases along with the surface area, which increases the volume of the adsorbent and increases the number of active sites, which improves the removal rate, and as a result, the removal percentage (Re% = 99.40863) of the MG dye. While (0.05) g has been found to be the ideal weight for adsorption in studies.

The appropriate equilibrium time to remove a given concentration of MG dye adsorbed by the adsorbent surface at a temperature of 25 °C, pH = 7, and an adsorbent surface constant weight of

0.05 g at a concentration of 1000 ppm was studied for different time periods ranging from 1 to 180 min, as shown in Fig. 7. It was found that the time required to reach equilibrium is 120 minutes, as the amount of dye absorbed increases rapidly at the beginning of the first minutes of the adsorption 198.8173, after which the increase is gradual until the time required to reach equilibrium. The reason for the rapid increase in the amount of dye adsorbed indicates that there are a large number of active centers at the beginning of the adsorption process that are unoccupied and sufficient for the adsorption of dyes. Thereafter, the adsorption process becomes slow and more difficult due to the preoccupation of all effective centers of the adsorbed surface with dye molecules [33].

Different amounts of the manufactured adsorbent surface were to see how they affected the adsorption of the MG dye, which would indicate the ideal tested adsorbent weight. To do this, different amounts of the gel produced (from 0.01g to 0.11g) were dipped into 10 mL of a 1000 ppm MG dye solution. The samples were shaken for 120 minutes at 25°C and 120 revolutions per

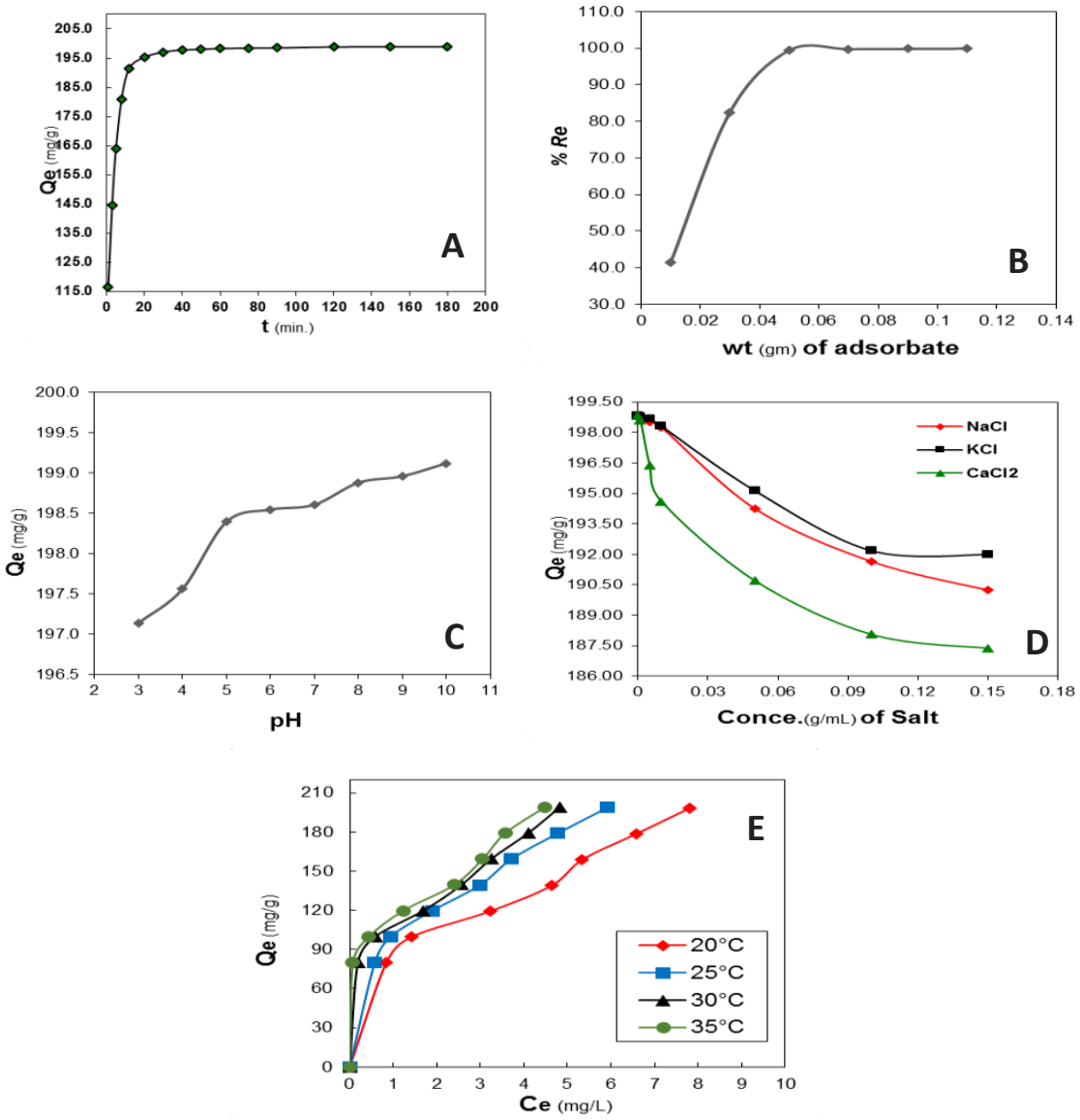

Fig. 7. (A) Effect of contact time, (B) Weight, (C)PH, (D)Salts on the adsorption of MG dye on the surface of the adsorbent compound (NaCMC-g-AAc)/COOH-MWCNTs and(E) Effect of Temperature

minute in a controlled apparatus. The solutions were then centrifuged at 6000 rpm for 15 minutes to separate them. Therefore, the ideal weight affecting the adsorption of the MG dye may be determined by plotting the amount of adsorbed substance versus the weight of the adsorbent surface. As shown in the Fig. 7.

The effect of pH on the MG dye adsorption process on the absorbent surface was studied at a concentration of 1000 ppm at pH values within the range (3-10) with constant conditions of temperature and equilibrium time. Through the results shown in Fig. 7, it was observed that the amount of MG dye adsorption on the surface of the adsorbent increases with the increase of the PH. The reason for this is that when the pH is high, the -COOH and OH groups will ionize and turn into negative groups, which means the surface of the adsorbent becomes negative. Which leads to electrostatic and static attraction between the positive dye molecules and the adsorbent surface, which increases the adsorption process, and the occurrence of repulsion between the negative ions on the adsorbent surface increases the swelling process, allowing the dye particles to spread within the overlay surface, which also increases the adsorption process .[34] When the pH is low, the H + ions will be very high in the solution, which leads to competition between them and the cationic dye molecules for the active sites, which reduces the adsorption process. The low pH leads to hydrogen bonding between the polymer chains and COOH-MWCNTs, which leads to That the surface is in a contraction state, which makes it difficult for the dye molecules to diffuse inside the adsorbent surface, as well as the repulsion between -COOH, OH groups present on the surface of the adsorbent and the positively charged dye. This makes it difficult for the molecules to reach the surface, which leads to a decrease in the adsorption process [35, 36].

The effect of salts on the adsorption process of MG dye on the Adsorbent surface was studied using different weights of CaCl, KCl and NaCl salts with constant conditions such as dye concentration, temperature, time and weight of the adsorbed composite surface. The results shown in Fig. 7 showed that the adsorption amount of MG dye on the surface of the adsorbent decrease with increasing salt concentration. The reason for this is due to the competition that occurs between the positive ions of the salts and the positive dye molecules on the active sites of the adsorbent surface, where these salts increase the solubility of the dye in the solution, which leads to the possibility that the ions from these salts bind to the active sites of the adsorbent [37]. In addition, there is another effect, which is that the negative ions of the salts will form a double complex with the dye molecules, and this compound is usually unable to absorb on the surface of the absorbent material, as it was observed that this effect of these salts when the absorption of MG dye decreases is in the following order: NaCl<KCl< $CaCl_2$.

Temperature significantly influences the adsorption process, as its modification can either reduce or augment the adsorbent surface's capacity to adsorb dyes from their aqueous solutions. As depicted in Fig. 7, the adsorption process escalates with increasing temperature. This suggests an endothermic nature of the adsorption process, where an elevation in temperature enhances the

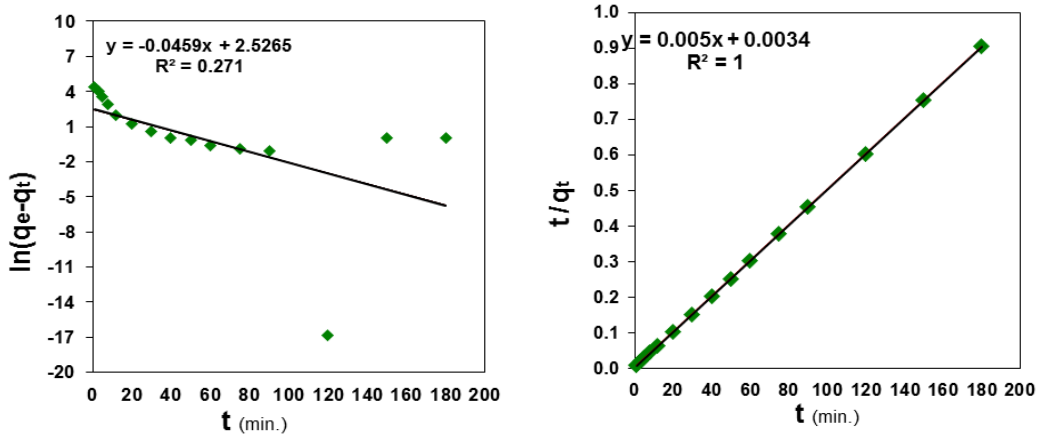

Fig. 8. a-The pseudo first-order adsorption MG dye b- the pseudo second-order adsorption MG

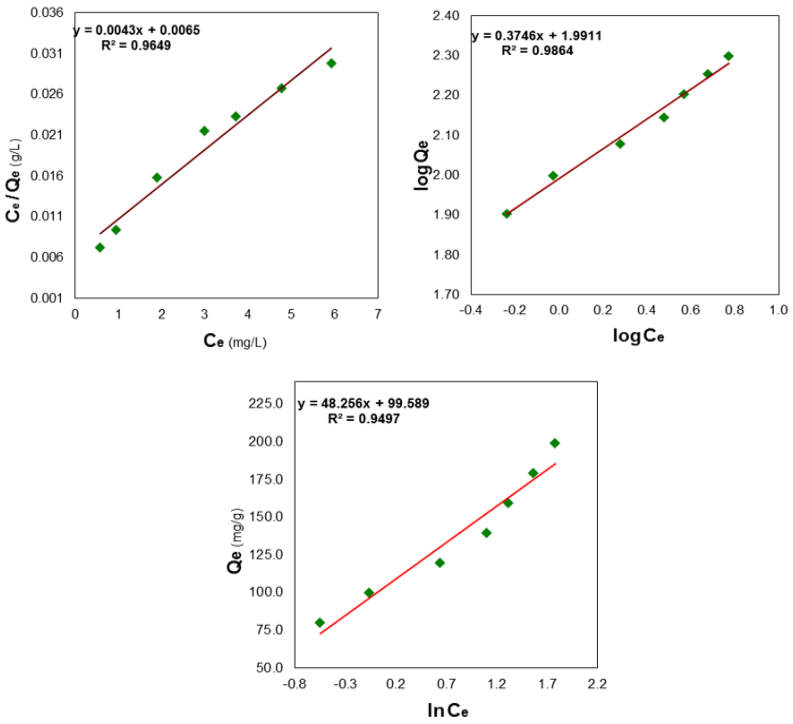

Fig. 9. Adsorption isotherm models for MG dye (A) Langmuir, (B) Freundlich, and (C) Temkin model

kinetic energy of the resultant dye molecules. Additionally, increased temperature causes an expansion in the adsorbent surface's internal structure, facilitating the diffusion of the adsorbed dye particles within the adsorbent surface pores. Therefore, dye particles initially spread on the pore surface and increasingly permeate deeper pores with rising temperature [27].

Furthermore, this study computes thermodynamic function values for their significance in elucidating the MG dye adsorption process on the overlaid adsorbent surface. The

Table1. Kinetic adsorption coefficients of (NaCMC-g-pAAc)/COOH-MWCNTs nanocomposite hydrogel.

Pseudo first order			Pseudo second order		
k_1	Q_e	R^2	k_2	Q_e	R^2
0.0459	12.509	0.2710	0.0074	200	1.0000

Table 2. Langmuir, Freundlich, and Temkin isotherm models for the MG adsorption

Model	*R²*		
Langmuir	0.9649	q_m	k_L
		232.558	0.662
Freundlich	0.9864	N	k_F
		2.669	97.972
Temkin	0.9497	B	k_T
		48.256	7.876

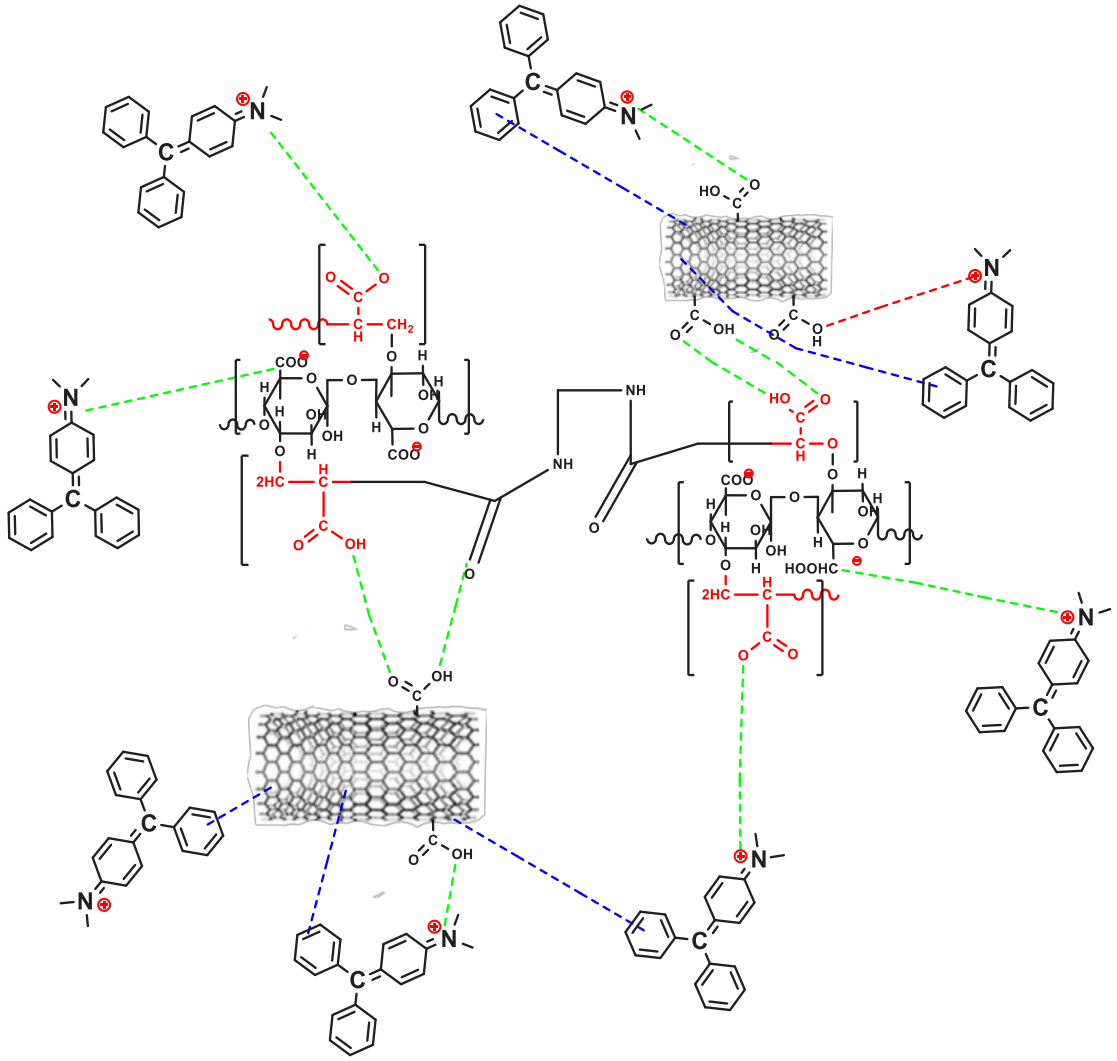

Fig. 10. Mechanism for (NaCMC-g-pAAc)/COOH-MWCNTs nanocomposite hydrogel and MG dye interaction

effect of temperature on the adsorption process was used to calculate thermodynamic function values (ΔG free energy, ΔH enthalpy, ΔS entropy). These thermodynamic functions are crucial in understanding the adsorption process as they provide a comprehensive description of the dye molecules' regularity nature resulting from molecular interactions, by measuring the change in entropy ΔS, and by gauging the change in enthalpy ΔH. The governing forces can be determined as either chemical or physical, in addition to establishing the reaction's direction [28].

The thermodynamic function values of the dye adsorption process imply that the positive enthalpy ΔH= 0.012(KJ/mol.) indicates an endothermic adsorption process. Simultaneously, the negative value of free energy ΔG= -15.409 (kJ/mol.) suggests spontaneous adsorption under the conducted conditions. The positive value indicative of the change in entropy ΔS= 51.709(kJ/mol.) suggests the adsorbed dye molecules are in a state of persistent and random motion [40]. The MG dye adsorption is also deemed a physical adsorption due to the ΔH value being less than (40 KJ/mol) [29].

The first and second-order false pseudo-models for MG dye absorption on the adsorbent surface were determined accurately (9). (R2) is significantly greater for the second-order incorrect model than for the first-order incorrect model,

indicating that the (MG) solution adsorption is first-order incorrect (Fig. 8). The percentage of dye released was also determined [30].

For adsorption isotherm experiments, MG dye concentrations ranged from 400 to 1000 mg/L. The effect of contact time and equilibrium concentration was evaluated at 25 °C. After the adsorption process, the aliquots were filtered and the concentration was measured with a UV-vis spectrophotometer at λmax 625 nm for the MG dye. The adsorption ratio and adsorption capacity (qe) were determined using Equations 2,3 respectively,and then the well-known isothermal equation models, Freundlich, Langmuir and Timken, were applied to the data obtained from the adsorption of MG dye onto the composite. Surface (NaCMC-g-pAAc/COOH-MWCNTs nanocomposite hydrogels) as shown in Table 2 and Fig. 9, where the Freindlich model showed a high agreement with the adsorption data at equilibrium, which is evident from the value of correlation coefficient (R^2) = 0.9864 for MG dye . Free isotherms indicate the homogeneous nature of the surface and that active sites are present on the superposition surface, which have equal energy, as indicated by the formation of a monolayer of adsorbed particles. The Freundlich isothermal model is valid for multilayer adsorption of a dense material on the surface of a heterogeneous absorbent material [31].

Fig. 10 illustrates the potential mechanism for the MG dye adsorption onto NaCMC-g-p AAc/COOH-MWCNTs. Both the hydrogel and the filler (COOH-MWCNTs) comprise carboxyl groups on their surfaces. Consequently, the (NaCMC-g-pAAc)/COOH-MWCNTs nanocomposite hydrogel's formation was facilitated by a robust hydrogen bond between the hydrogel and o-MWCNTs. Adsorption studies (effect of solution pH) demonstrated that high MG adsorption onto the (NaCMC-g-pAAc)/COOH-MWCNTs nanocomposite hydrogel surface was realized within a pH range of 5–10. This outcome indicates a powerful electrostatic attraction between the adsorbent and the MG dye molecules. The surface of the (NaCMC-g-pAAc)/COOH-MWCNTs nanocomposite hydrogel, abundant with carboxyl groups, dissociated into carboxylate anions, thus inducing the attraction of positively charged MG dye molecules. Furthermore, the π-π stacking interaction between MG and COOH-MWCNTs could also contribute to the (NaCMC-g-pAAc)/ COOH-MWCNTs nanocomposite hydrogel's high sorption capacity [32].

CONCLUSION

Graft co-polymerization was used to synthesize hydrogel and nanocomposite. Analytical methods confirmed COOH-MWCNTs in the hydrogel network. TG and SEM examination showed the polymeric hydrogel matrix had the correct COOH-MWCNT distribution. FTIR research showed that COOH-MWCNTs reduced the absorption intensity of NaCMC-g-pAAc hydrogel, confirming internal hydrogen bonding among carboxyl groups. (NaCMC-g-pAAc)/COOH-MWCNTs nanocomposite hydrogel was used to batch-adsorb MG from aqueous solution. Initial pH, adsorbent dosage, contact time, and equilibrium concentration affected MG adsorption. Pseudo-second-order and Freundlich models best captured the sorption process. The Freundlich isotherm model showed that (NaCMC-g-pAAc)/COOH-MWCNTs nanocomposite hydrogel can adsorb MG dye at 198.8173 mg/g at 25°C under ideal conditions. Regeneration experiments showed that the produced adsorbent may be used repeatedly without losing adsorption capability. Adsorption investigations demonstrated that electrostatic interaction drove sorption. This study's NaCMC-pAAc/COOH-MWCNTs have wastewater treatment potential.

CONFLICT OF INTEREST

The authors declare that there is no conflict of interests regarding the publication of this manuscript.

REFERENCES

1. Ma J, Yu F, Zhou L, Jin L, Yang M, Luan J, et al. Enhanced Adsorptive Removal of Methyl Orange and Methylene Blue from Aqueous Solution by Alkali-Activated Multiwalled Carbon Nanotubes. ACS Applied Materials and Interfaces. 2012;4(11):5749-5760.
2. Wu C-H. Adsorption of reactive dye onto carbon nanotubes: Equilibrium, kinetics and thermodynamics. Journal of Hazardous Materials. 2007;144(1-2):93-100.
3. Aljeboree AM, Abdulrazzak FH, Saleh ZM, Abbas HA, Alkaim AF. Eco-Friendly Adsorption of Cationic (Methylene Blue) and Anionic (Congo Red) Dyes from Aqueous Solutions Using Sawdust. RAiSE-2023; 2024/01/24: MDPI; 2024.
4. Mishra AK, Arockiadoss T, Ramaprabhu S. Study of removal of azo dye by functionalized multi walled carbon nanotubes. Chemical Engineering Journal. 2010;162(3):1026-1034.
5. Cheng S, Zhang L, Ma A, Xia H, Peng J, Li C, Shu J. Comparison of activated carbon and iron/cerium modified activated carbon to remove methylene blue from wastewater. Journal of Environmental Sciences. 2018;65:92-102.

6. Aljeboree AM, Al-Baitai AY, Abdalhadi SM, Alkaim AF. Investigation Study of Removing Methyl Violet Dye From Aqueous Solutions Using Corn-Cob as A Source of Activated Carbon. Egyptian Journal of Chemistry. 2021;0(0):0-0.
7. Mohamed A, Ghobara MM, Abdelmaksoud MK, Mohamed GG. A novel and highly efficient photocatalytic degradation of malachite green dye via surface modified polyacrylonitrile nanofibers/biogenic silica composite nanofibers. Separation and Purification Technology. 2019;210:935-942.
8. Radia ND, Mahdi AB, Mohammed GA, Sajid A, Altimari US, Shams MA, et al. Removal of Rose Bengal Dye from Aqueous Solution using Low Cost (SA-g-PAAc) Hydrogel: Equilibrium and Kinetic Study. INTERNATIONAL JOURNAL OF DRUG DELIVERY TECHNOLOGY. 2022;12(03):957-960.
9. Othman N, Raja Sulaiman RN, Rahman HA, Noah NFM, Jusoh N, Idroas M. Simultaneous extraction and enrichment of reactive dye using green emulsion liquid membrane system. Environmental Technology. 2018;40(11):1476-1484.
10. Tehrani-Bagha AR, Mahmoodi NM, Menger FM. Degradation of a persistent organic dye from colored textile wastewater by ozonation. Desalination. 2010;260(1-3):34-38.
11. Yao Y, Bing H, Feifei X, Xiaofeng C. Equilibrium and kinetic studies of methyl orange adsorption on multiwalled carbon nanotubes. Chemical Engineering Journal. 2011;170(1):82-89.
12. Chang PR, Zheng P, Liu B, Anderson DP, Yu J, Ma X. Characterization of magnetic soluble starch-functionalized carbon nanotubes and its application for the adsorption of the dyes. Journal of Hazardous Materials. 2011;186(2-3):2144-2150.
13. Eskandarian L, Arami M, Pajootan E. Evaluation of Adsorption Characteristics of Multiwalled Carbon Nanotubes Modified by a Poly(propylene imine) Dendrimer in Single and Multiple Dye Solutions: Isotherms, Kinetics, and Thermodynamics. Journal of Chemical & Engineering Data. 2014;59(2):444-454.
14. Zheng S, Guo H, Yang F, Hong B. Novel organic dye sorbent: synthesis and adsorption properties of multi-walled carbon nanotubes modified with gallic amide units. Desalination and Water Treatment. 2015;57(26):12264-12273.
15. Ghobadi J, Arami M, Bahrami H, Mahmoodi NM. Modification of carbon nanotubes with cationic surfactant and its application for removal of direct dyes. Desalination and Water Treatment. 2013;52(22-24):4356-4368.
16. Wang S, Ng CW, Wang W, Li Q, Li L. A Comparative Study on the Adsorption of Acid and Reactive Dyes on Multiwall Carbon Nanotubes in Single and Binary Dye Systems. Journal of Chemical and Engineering Data. 2012;57(5):1563-1569.
17. Wu C-H. Studies of the equilibrium and thermodynamics of the adsorption of Cu^{2+} onto as-produced and modified carbon nanotubes. Journal of Colloid and Interface Science. 2007;311(2):338-346.
18. Gong J-L, Wang B, Zeng G-M, Yang C-P, Niu C-G, Niu Q-Y, et al. Removal of cationic dyes from aqueous solution using magnetic multi-wall carbon nanotube nanocomposite as adsorbent. Journal of Hazardous Materials. 2009;164(2-3):1517-1522.
19. Kierkowicz M, Pach E, Santidrián A, Sandoval S, Gonçalves G, Tobías-Rossell E, et al. Comparative study of shortening and cutting strategies of single-walled and multi-walled carbon nanotubes assessed by scanning electron microscopy. Carbon. 2018;139:922-932.
20. Van Khu L, Duc Manh T. Adsorption of methylene blue from aqueous solutions using activated carbon derived from coffee husks. Journal of Science, Natural Science. 2015;60(4):32-43.
21. Chiang Y-C, Lin W-H, Chang Y-C. The influence of treatment duration on multi-walled carbon nanotubes functionalized by H_2SO_4/HNO_3 oxidation. Applied Surface Science. 2011;257(6):2401-2410.
22. Mahdi ZS, Aljeboree AM, Rasen FA, Salman NAA, Alkaim AF. Synthesis, Characterization, and Regeneration of Ag/TiO_2 Nanoparticles: Photocatalytic Removal of Mixed Dye Pollutants. RAiSE-2023; 2024/01/26: MDPI; 2024.
23. Hosseinzadeh S, Hosseinzadeh H, Pashaei S, Khodaparast Z. Synthesis of magnetic functionalized MWCNT nanocomposite through surface RAFT co-polymerization of acrylic acid and N-isopropyl acrylamide for removal of cationic dyes from aqueous solutions. Ecotoxicology and Environmental Safety. 2018;161:34-44.
24. Salikova NS, Bektemissova AU, Nazarova VD, Begenova BE, Ostafeichuk NV. Preparation of mixed hydrogels based on biopolymers and the study of their rheological properties. Periódico Tchê Química. 2020;17(35):23-40.
25. Aljeboree AM, Fared RW, Al-wahed HMA, Jawad MA, Alkaim AF. Role of SA-g-(PAA-co-AM)/CdS Hydrogel: As Photocatalytic for Decolonization Methyl Red Dye as a Pollutant from Aqueous Solution. International journal of pharmaceutical quality assurance. 2023;14(01):171-174.
26. Radia ND, Aljeboree AM, Mahdi AB, Alkai AF. Eco-friendly Synthesis of Hydrogel Nano-composites for Removal of Pollutants as a Model Rose Bengal Dye. International journal of drug delivery technology. 2022;12(04):1527-1530.
27. Shen J, Yan B, Li T, Long Y, Li N, Ye M. Mechanical, thermal and swelling properties of poly(acrylic acid)–graphene oxide composite hydrogels. Soft Matter. 2012;8(6):1831-1836.
28. Al-Ghouti MA, Khraisheh MAM, Allen SJ, Ahmad MN. The removal of dyes from textile wastewater: a study of the physical characteristics and adsorption mechanisms of diatomaceous earth. Journal of Environmental Management. 2003;69(3):229-238.
29. Thakur S, Pandey S, Arotiba OA. Sol-gel derived xanthan gum/silica nanocomposite—a highly efficient cationic dyes adsorbent in aqueous system. International Journal of Biological Macromolecules. 2017;103:596-604.
30. Makhado E, Pandey S, Nomngongo PN, Ramontja J. Fast microwave-assisted green synthesis of xanthan gum grafted acrylic acid for enhanced methylene blue dye removal from aqueous solution. Carbohydrate Polymers. 2017;176:315-326.
31. Atta A, Akl MA, Youssef AM, Ibraheim MA. Superparamagnetic Core-Shell Polymeric Nanocomposites for Efficient Removal of Methylene Blue from Aqueous Solutions. Adsorption Science & Technology. 2013;31(5):397-419.
32. Blanton TN, Majumdar D. Characterization of X-ray irradiated graphene oxide coatings using X-ray diffraction, X-ray photoelectron spectroscopy, and atomic force microscopy. Powder Diffraction. 2013;28(2):68-71.